A PARTICLE SUSPENSION MODEL FOR NANOSUSPENSIONS ELECTROSPINNING

by

Lan XU*

National Engineering Laboratory for Modern Silk, College of Textile and Clothing Engineering, Soochow University, Suzhou, China

Original scientific paper
https://doi.org/10.2298/TSCI1804707X

Polymeric composite nanofibers have been fabricated simply by the electrospinning of polymeric solutions containing a wide variety of suspended inclusions such as nanoparticles and nanotubes. The electrospinning process for fabrication of composite nanofibers is a multi-phase and multi-physics process. In this paper, a modified particle suspension model for electrospinning nanosuspensions is established to research the electrospinning process. The model can offer in-depth insight into physical understanding of the complex process which can not be fully explained experimentally.

Key words: *composite nanofibers, electrospinning, nanosuspensions, velocity distribution, mathematical model*

Introduction

Electrospinning has attracted much attention in recent years due to its versatility and potential for applications such as photoelectric [1], electronics [2], catalysis [3], drug delivery [4, 5], and scaffolds for tissue engineering [6-8]. Polymeric composite nanofibers [9] have also been fabricated by the electrospinning of polymeric solutions containing a wide variety of inclusions such as nanoparticles [10-12] and nanotubes [13-16]. The electrospinning process for fabrication of composite nanofibers is a multi-phase and multi-physics process. The electrospinning process has been studied experimentally and theoretically [17-20]. In recent years, many experimental studies have been conducted to understand the electrospinning process and a number of mathematical models have been developed for research mechanical mechanism of the process [21-25].

Particle suspension occurs in a wide variety of natural and man-made materials. Particle migration in suspension flows is important in a variety of scientific and engineering applications such as the transport of sediments, chromatography, and composite materials processing [26]. Particle shape plays a pivotal role in determining the distributions of particle orientation, concentration, and velocity in suspension flows. Slender particle is different from spherical particle, since it is orientable while the latter is isotropic. Slender particle suspension flow always show non-isotropic properties, such as huge extensional viscosity, the first normal stress difference and the second normal stress difference.

The distributions of particle orientation, concentration, and velocity are main topics in the previous investigation of particle suspensions [27]. Leighton and Acrivos [28] proposed

* Author's, e-mail: lanxu@suda.edu.cn

a particle diffusive model, in which the driving force perpendicular to the shear plane is supposed to result from the effects of spatially varying interparticle interaction and effective viscosity. Brady presented a suspension balance model [29], which is based on the conservation of mass and momentum for both particle and suspension phases. Phillips *et al.* [30] adopted Leighton's scaling arguments and proposed a diffusive flux equation to describe the time evolution of the solid concentration based on the two-body interaction model. The particle flux is considered to be a balance between a contribution due to spatially varying collision frequencies and an opposite contribution due to spatially varying viscosity. Koh *et al.* [31] measured the velocity and concentration profiles for the flow of concentrated suspensions, and found that the concentration becomes more uniform with increasing flow rate and with decreasing the average concentration. Olson [32] investigated the distribution of fiber concentration and observed a maximum peak of concentration between the linear and constant concentration regions. Lin and Shen [27] and Lin *et al.* [33] investigated theoretically and numerically the orientation, concentration and velocity distribution of fibers in the turbulent channel flows. These theoretical and numerical analyses can offer in-depth insight into physical understanding of the particle migration in suspension flows which cannot be fully explained experimentally.

The electrospun solutions for fabrication of composite nanofibers are nanoparticle suspensions, and the electrospinning process is a multi-phase and multi-physics process. In this paper, a modified particle suspension model for electrospinning nanosuspensions, which plays a pivotal role in determining the nanofiber quality, is established to research the electrospinning process. The model can offer in-depth insight into physical understanding of the complex process which can not be fully explained experimentally, and can be used to optimize and control the electrospinning parameters.

Particle suspension model

Instantaneous equation of particle suspension flow

The electrospinning process for fabrication of composite nanofibers is a particle suspension flow. The particle suspension flow is assumed to be an incompressible and steady--state. The governing equations of particle suspension are derived by considering balance equations for both the suspension as a whole and for the particle phase [29]. In the proceeding sections, conservation of mass and momentum for the particle suspensions can be obtained by averaging those quantities over all phases in a unit volume, *V*, as shown in fig. 1.

Spherical particle suspension flow

The instantaneous continue and momentum equations of spherical particle suspension flow in electrospinning process are [22]:

– continue equation

$$\frac{\partial u_i}{\partial x_i} = 0 \tag{1}$$

where u_i is the velocity.

– momentum equation

$$\rho u_j \frac{\partial u_i}{\partial x_j} = -\frac{\partial p}{\partial x_i} + \mu \frac{\partial^2 u_i}{\partial^2 x_j} + q_e E_i + \varepsilon_p E_j \frac{\partial E_i}{\partial x_j} \tag{2}$$

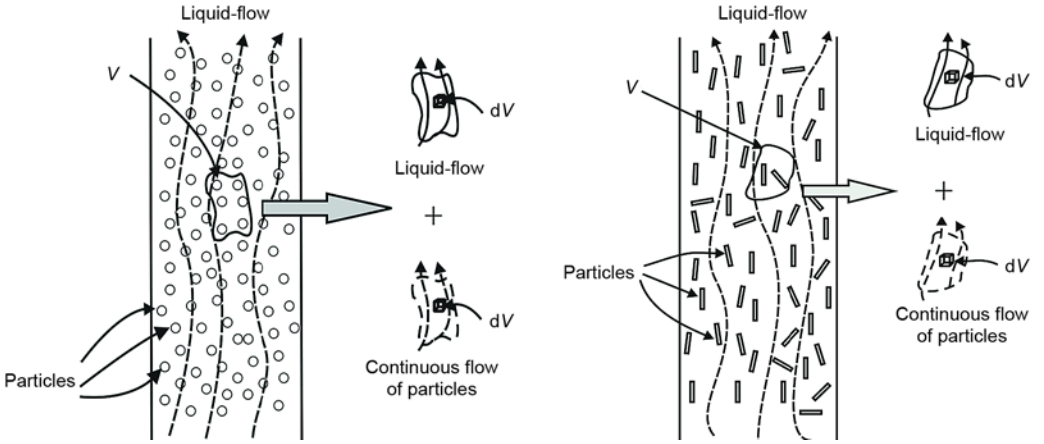

Figure 1. Schematic representation of particle suspension flow in electrospinning process; (a) spherical particle, (b) slender particle

where p is the pressure, μ – the dynamic viscosity of the particle suspension flow, q_e – the electric charge, E – the electric field, and ε_p – the material module.

Slender particle suspension flow

The instantaneous continue and momentum equations of slender particle suspension flow in electrospinning process are as follows [22, 34]:
– continue equation

$$\frac{\partial u_i}{\partial x_i}=0 \tag{3}$$

– momentum equation

$$\rho u_j \frac{\partial u_i}{\partial x_j}=-\frac{\partial p}{\partial x_i}+\mu\frac{\partial^2 u_i}{\partial^2 x_j}+\mu_f \frac{\partial}{\partial x_j}\left[\left(a_{ijkl}-\frac{1}{3}I_{ij}a_{kl}\right)\varepsilon_{kl}\right]+q_e E_i+\varepsilon_p E_j \frac{\partial E_i}{\partial x_j} \tag{4}$$

where ρ is the density of the suspending flow, ε_{ij} – the tensor of rate of strain, and μ_f – the apparent viscosity of the suspension. Also

$$\varepsilon_{ij}=\frac{\dfrac{\partial u_i}{\partial x_j}+\dfrac{\partial u_j}{\partial x_i}}{2} \tag{5}$$

$$\mu_f=\frac{\pi n\mu l^3}{6\ln(2r)} \tag{6}$$

where n is the number of slender particles per unit volume, l – the slender particle half-length, and r – the slender particle aspect-ratio which is the ratio of length to diameter of a slender particle. The a_{ij} and a_{ijkl} are the second- and fourth-orientation tensor of a slender particle, and can be defined, according to the following model, respectively, [35]:

$$a_{ij} = \oint q_i q_j \psi(\boldsymbol{q}) \mathrm{d}\boldsymbol{q} \tag{7}$$

$$a_{ijkl} = \oint q_i q_j q_k q_l \psi(\boldsymbol{q}) \mathrm{d}\boldsymbol{q} \tag{8}$$

where q_i is a unit vector parallel to the slender particle's axis, $\psi(\boldsymbol{q})$ – the probability distribution function for slender particle orientation at any positions.

Based on the definition of $\psi(\boldsymbol{q})$, $\psi(\boldsymbol{q})$ satisfies the equation of conservation:

$$\frac{\partial \psi}{\partial t} + u_j \frac{\partial \psi}{\partial x_j} = -\frac{\partial(\psi \dot{q}_j)}{\partial q_j} \tag{9}$$

where $\dot{q}_j$ is the slender particle angular velocity and given as [36]:

$$\dot{q}_i = -\omega_{ij} q_j + \lambda \varepsilon_{ij} q_j - \lambda \varepsilon_{kl} q_k q_l q_i \tag{10}$$

where ω_{ij} is the vorticity tensor.

$$\omega_{ij} = \frac{\dfrac{\partial u_j}{\partial x_i} + \dfrac{\partial u_i}{\partial x_j}}{2} \tag{11}$$

$$\lambda = \frac{r^2 - 1}{r^2 + 1} \tag{12}$$

Equation for turbulent slender particle suspension

The instantaneous velocity, pressure, tensor of rate of strain, and orientation tensor as sum of the mean and fluctuation quantities can be written:

$$u_i = \overline{u}_i + u'_i, \quad p = \overline{p} + p', \quad \varepsilon_{ij} = \overline{\varepsilon}_{ij} + \varepsilon'_{ij}, \quad a_{ij} = \overline{a}_{ij} + a'_{ij}, \quad a_{ijkl} = \overline{a}_{ijkl} + a'_{ijkl} \tag{13}$$

The a'_{ij} and a'_{ijkl} are dependent on the rotation angle of slender particle, ε'_{ij} is dependent on the spatial position of slender particle. Therefore, the correlations of $\overline{a'_{kl}\varepsilon'_{kl}}$ and $\overline{a'_{ijkl}\varepsilon'_{kl}}$ equal to zero. Substituting eq. (13) into eq. (4) and taking the average yields:

$$\rho \overline{u}_j \frac{\partial \overline{u}_i}{\partial x_j} = -\frac{\partial \overline{p}}{\partial x_i} + \mu \frac{\partial^2 \overline{u}_i}{\partial^2 x_j} + \rho \frac{\partial \overline{u'_i u'_j}}{\partial x_j} + \mu_f \frac{\partial}{\partial x_j}\left[\left(\overline{a}_{ijkl} - \frac{1}{3} I_{ij} \overline{a}_{kl}\right)\overline{\varepsilon}_{kl}\right] + q_\mathrm{e} E_i + \varepsilon_p E_j \frac{\partial E_i}{\partial x_j} \tag{14}$$

Equation (14) is the mean motion equation of turbulent slender particle suspensions.

Equation for the particle phase

According to the suspension balance model [29], the conservations of mass and momentum for the particle phase are obtained by averaging the equations of conservation of mass and Cauchy's equations of motion over the particles.

– continue equation

$$\frac{\partial \phi}{\partial t} + \nabla(\phi \overline{\boldsymbol{u}}_p) = 0 \tag{15}$$

– momentum equation

$$\rho_p \phi \frac{\mathrm{d}\bar{\boldsymbol{u}}_p}{\mathrm{d}t} = (\rho_p - \rho)\mathrm{g}\phi + \boldsymbol{F}_p + \nabla \boldsymbol{\tau}_p + q_\mathrm{e}\boldsymbol{E} + \varepsilon_p (\nabla \boldsymbol{E})\boldsymbol{E} \tag{16}$$

where ρ_p is the particle density, $\bar{\boldsymbol{u}}_p$ – the particle-phase average velocity, g – the gravitational acceleration, ϕ – the volume fraction of the particle, and $\boldsymbol{E}$ – the electric field. The $\boldsymbol{F}_p$ is the mean Stokes drag force on any particle in the suspension flow, which may be modeled as analogous to the drag in sedimentation and set:

$$\boldsymbol{F}_p = -6\pi n \mu a f(\phi)^{-1}(\bar{\boldsymbol{u}}_p - \boldsymbol{u}) \tag{17}$$

where a is the dimension parameter of the particles. The hindered setting function, $f(\phi)$, represents the mean mobility of the particle phase, and thus $f(\phi)^{-1}$ is the mean resistance, which can be determined by the sedimentation hindrance function described in [37].

$$f(\phi) = \frac{1-\phi}{\phi_\mathrm{m}}(1-\phi)^{\alpha-1} \tag{18}$$

where ϕ_m is the maximum packing particle volume fraction, α – the parameter given by Richardson and Zaki [37] as $\alpha = 2 - 5$, τ_p – the particle contribution to the bulk stress, and is suggested by Morris and Brady [38] for shear flows:

$$\tau_p = -\mu\mu_n(\phi)\dot{\gamma}Q + \mu\mu_p(\phi)[\nabla\boldsymbol{u} + (\nabla\boldsymbol{u})^T] \tag{19}$$

$$\mu_n(\phi) = \frac{K_n\left(\dfrac{\phi}{\phi_\mathrm{m}}\right)^2}{\left(\dfrac{1-\phi}{\phi_\mathrm{m}}\right)^2} \tag{20}$$

$$\mu_p(\phi) = 2.5\phi_\mathrm{m}\frac{\dfrac{\phi}{\phi_\mathrm{m}}}{\dfrac{1-\phi}{\phi_\mathrm{m}}} + \frac{K_s\left(\dfrac{\phi}{\phi_\mathrm{m}}\right)^2}{\left(\dfrac{1-\phi}{\phi_\mathrm{m}}\right)^2} \tag{21}$$

where K_p and K_s are rheological fitting parameters, with $K_p = 0.75$ and $K_s = 0.1$ to match experimental data [39]. The $\dot{\gamma}$ is the shear rate and gives the stress its dependence on the strength to the local flow. The Q is the tensor parameter and captures the anisotropy of the normal stress with the following form [40]

$$Q = \begin{pmatrix} 1 & 0 & 0 \\ 0 & 0.8 & 0 \\ 0 & 0 & 0.5 \end{pmatrix} \tag{22}$$

Finite volume method

The finite volume method is widely used to solve convective-diffusive problems mainly due to its conservative property and its lucid physical interpretation [41]. In the finite volume method, for instance, in the most popular SIMPLER algorithm [42], a staggered mesh in which the pressure nodes are located between the velocity nodes must be used to avoid a checkerboard type pressure field, so that one ends up with four different sets of control volumes: three for the three velocity components, one for the pressure and any other variables (*i. e.* temperature) to be solved.

All field variables of the equations can be written as a general form Φ. The integrals of these field variables can be evaluated, with the help of an interpolation scheme to obtain the following discrete equation:

$$a_C^t \Phi_C^t = \sum a_{nb}^t \Phi_{nb}^t + a_C^0 \Phi_C^{t-\Delta t} + b^t \tag{23}$$

where the subscript *C* denotes the current node, the subscript *nb* represents all neighboring nodes to *C*, the superscript *t* indicates the currents time, Δt is the time step, and the coefficients are found from the grid geometry and the current kinematics.

The discrete equation for pressure is obtained by discretizing the continue equation [42]:

$$a_C^t p_C^t = \sum a_{nb}^t p_{nb}^t + b^t \tag{24}$$

According to the particle suspension model presented, the finite volume method will be used in the solver, and the SIMPLEC algorithm enforces mass conservation and achieves pressure-velocity coupling. In future, we will apply computational fluid mechanics to simulate the jet numerically for researching the effect of slender particle on the electrospinning process.

Conclusion

In this paper, a modified particle suspension model, derived from Lin's turbulent fiber suspension model [22] is presented to research mechanical mechanism of the electrospinning process for fabrication of composite nanofibers. The model can offer in-depth insight into physical understanding of the complex electrospinning process, and be used to optimize and control the electrospinning parameters. Based on the model, numerical simulation and experiment verification will be carried out to research the effect of slender particle on the electrospinning process in future. The model will be further ameliorated according to numerical results and experimental data.

Acknowledgment

The work is supported financially by National Natural Science Foundation of China (Grant No. 11672198), PAPD (A Project Funded by the Priority Academic Program Development of Jiangsu Higher Education Institutions), Natural Science Foundation of the Jiangsu Higher Education Institutions of China (Grant No. 14KJA130001), and Six Talent Peaks Project of Jiangsu Province (Grant No. GDZB-050).

References

[1] Vannikov, A.V., *et al.*, Photoelectric, Nonlinear Optical and Photorefractive Properties of Polymer/Carbon Nanotube Composites, *Carbon, 49* (2011), 1, pp. 311-319

[2] Zhang, H. Y., *et al.*, Li4Ti5O12/CNTs Composite Anode Material for Large Capacity and High-Rate Lithium Ion Batteries Original, *International Journal of Hydrogen Energy*, *39* (2014), 28, pp. 16096-16102

[3] Ramakrishna, S. U. B., *et al.*, Nitrogen Doped CNTs Supported Palladium Electrocatalyst for Hydrogen Evolution Reaction in PEM Water Electrolyser, *International Journal of Hydrogen Energy*, *41* (2016), 45, pp. 20447-20454

[4] Xu, L., *et al.*, Fabrication and Characterization of Chinese Drug-Loaded Nanoporous Materials, *Journal of Nano Research*, *27* (2014), Mar., pp.103-109

[5] Nguyen, T. T. T., *et al.*, Porous Core/Sheath Composite Nanofibers Fabricated by Coaxial Electrospinning as a Potential Mat for Drug Release System, *International Journal of Pharmaceutics*, *439* (2012), 1-2, pp. 296-306

[6] Mehrasa M., *et al.*, Electrospun Aligned PLGA and PLGA/Gelatin Nanofibers Embedded with Silica Nanoparticles for Tissue Engineering, *International Journal of Biological Macromolecules*, *79* (2015), Aug., pp. 687-695

[7] Sun, Z. Y., *et al.*, Characterization and Antibacterial Properties of Porous Fibers Containing Silver Ions, *Applied Surface Science*, *387* (2016), Nov., pp. 828-838

[8] Mikael, P. E., Nukavarapu, S. P., Functionalized Carbon Nanotube Composite Scaffolds for Bone Tissue Engineering: Prospects and Progress, *Journal of Biomaterials & Tissue Engineering*, *1* (2011), 1, pp. 76-85

[9] Sawicka, K. M., *et al.*, Electrospun Composite Nanofibers for Functional Applications, *Journal of Nanoparticle Research*, *8* (2006), 6, pp. 769-781

[10] Hamlett, C. A. E., *et al.*, Electrospinning Nanosuspensions Loaded with Passivated Au Nanoparticles, *Tetrahedron*, *64* (2008), 36, pp. 8476-8483

[11] Simon, Y. R. L., *et al.*, A Novel Route for the Preparation of Gold Nanoparticles in Polycaprolactone Nanofibers, *Journal of Nanomaterials*, *2015* (2015), ID 485121

[12] Wang, J., *et al.*, Facile Fabrication of Gold Nanoparticles-Poly(Vinyl Alcohol) Electrospun Water-Stable Nanofibrous Mats: Efficient Substrate Materials for Biosensors, *ACS Applied Materials and Interfaces*, *4* (2012), 4, pp. 1963-1971

[13] Song, Y. H., *et al.*, Preparation and Characterization of Highly Aligned Carbon Nanotubes/Polyacrylonitrile Composite Nanofibers, *Polymers*, *9* (2017), 1, pp. 1-13

[14] Kaseem, M., *et al.*, Fabrication and Materials Properties of Polystyrene/Carbon Nanotube (PS/CNT) Composites: A review, *European Polymer Journal*, *79* (2016), June, pp. 36-62

[15] Aqeel, S.M., *et al.*, Poly (Vinylidene Fluoride) /Poly (Acrylonitrile)-Based Superior Hydrophobic Piezoelectric Solid Derived by Aligned Carbon Nanotube in Electrospinning: Fabrication, the Phase Conversion and Surface Energy, *RSC Advances*, *5* (2015), 93, pp. 76383-76391

[16] Song, Y. H., Xu, L., Permeability, Thermal and Wetting Properties of Aligned Composite Nanofiber Membranes Containing Carbon Nanotubes, *International Journal of Hydrogen Energy*, *42* (2017), 31, pp. 19961-19966

[17] Xu, L., *et al.*, Effect of Humidity on the Surface Morphology of a Charged Jet, *Heat Transfer Research*, *44* (2013), 5, pp. 441-445

[18] Tang, X. P., *et al.*, Effect of Flow Rate on Diameter of Electrospun Nanoporous Fibers, *Thermal Science*, *18* (2014), 5, pp. 1439-1441

[19] Pratyush, D., *et al.*, Experimental and Theoretical Investigations of Porous Structure Formation in Electrospun Fibers, *Macromolecules*, *40* (2007), 21, pp. 7689-7694

[20] Zhao, J. H., *et al.*, Experimental and Theoretical Study on the Electrospinning Nanoporous Fibers Process, *Materials Chemistry and Physics*, *170* (2016), Feb., pp. 294-302

[21] Xu, L., *et al.*, Numerical Simulation for the Single-Bubble Electrospinning Process, *Thermal Science*, *19* (2015), 4, pp. 1255-1259

[22] Xu, L., *et al.*, A Multi-Phase Flow Model for Electrospinning Process, *Thermal Science*, *17* (2013), 5, pp. 1299-1304

[23] Xu, L., *et al.*, Theoretical Model for the Electrospinning Nanoporous Materials Process, *Computers and Mathematics with Applications*, *64* (2012), 5, pp. 1017-1021

[24] Fan, C., *et al.*, Fluid-Mechanic Model for Fabrication of Nanoporous Fibers by Electrospinnng, *Thermal Science*, *21* (2017), 4, pp. 1621-1625

[25] Xu, L., *et al.*, Numerical Simulation of a Two-Phase Flow in the Electrospinning Process, *International Journal of Numerical Methods for Heat and Fluid Flow*, *24* (2014), 8, pp. 1755-1761

[26] Fang, Z. W., *et al*., Flow-Aligned Tensor Models for Suspension Flows, International Journal of Multiphase Flow, 28 (2002), 1, pp. 137-166
[27] Lin, J. Z., Shen S. H., A New Formula for Predicting the Velocity Distribution in the Turbulent Fiber Suspensions of a Channel Flow, *Fibers and Polymers, 11* (2010), 3, pp. 438-447
[28] Leighton, D., Acrivos, A., The Shear-Induced Migration of Particles in Concentrated Suspensions, *Journal of Fluid Mechanics, 181* (1987), Aug., pp. 415-439
[29] Nott, P. R., Brady, J. F., Pressure-Driven Flow of Suspensions: Simulation and Theory, *Journal of Fluid Mechanics, 275* (1994), Sep., pp. 157-199
[30] Phillips, R. J., *et al.,* A Constitutive Equation for Concentrated Suspension that Accounts for Shear-induced Particle Migration, *Physics of Fluids A Fluid Dynamics, 4* (1992), 1, pp. 30-40
[31] Koh, C. J., *et al.,* An Experimental Investigation of Concentrated Suspension Flows in a Rectangular channel, *Journal of Fluid Mechanics, 266* (1994), May, pp. 1-32
[32] Olson, J. S., The Effect of Fiber Length on Passage Through Narrow Apertures, Ph. D. dissertation, University of British Columbia, Vancouver, Canada, 1996
[33] Lin, J. Z., *et al.,* New Equation of Turbulent Fiber Suspensions and its Solution and Application to the Pipe Flow, *Chinese Physics, 14* (2005), 6, pp. 1185-1192
[34] Batchelor, G. K., The Stress Generated in a Non-Dilute Suspension of Elongated Particles by Pure Straining Motion, *Journal of Fluid Mechanics, 46* (1971), 4, pp. 813-829
[35] Hinch, E. J., Leal, L. G., Constitutive Equations in Suspension Mechanics, Part II, Approximate Forms for a Suspension of Rigid Particles Affected by Brownian Rotations, *Journal of Fluid Mechanics, 76* (1976), 1, pp. 187-208
[36] Cintra, J. S., Tucker, C. L., Orthotropic Closure Approximations for Flow-Induced Fiber Orientation, *Journal of Rheology, 39* (1995), 6, pp. 1095-1122
[37] Richardson, J. F., Zaki, W. N., Sedimentation and Fluidization: Part I, *Transactions of the Institution of Chemical Engineers, 32* (1954), Jan., pp. 35-47
[38] Morris, J. F., Brady, J. F., Pressure-Driven Flow of a Suspension: Buoyancy Effects, *International Journal of Multiphase Flow, 24* (1998), 1, pp. 105-130
[39] Miller, R. M., Morris, J. F., Normal Stress-Driven Migration and Axial Development in Pressure-Driven Flow of Concentrated Suspensions, *Journal of Non-Newtonian Fluid Mechanics, 135* (2006), 2-3, pp. 149-165
[40] Zarraga, I. E., *et al.,* The Characterization of the Total Stress of Concentrated Suspensions of Noncolloidal Spheres in Newtonian Fluids, *Journal of Rheology, 42* (2000), 2, pp. 185-220
[41] Na, Y., Yoo, J. Y., A Finite Volume Technique to Simulate the Flow of a Viscoelastic Fluid, *Computational Mechanics, 8* (1991), 1, pp. 43-55
[42] Patankar, S. V., *Numerical Heat Transfer and Fluid Flow*, Hemisphere Publishing, New York, USA, 1980

Paper submitted: Juy 5, 2017
Paper revised: September 30, 2017
Paper accepted: September 30, 2017